JOURNAL OF NEUROTRAUMA 31:425–436 (March 1, 2014)

DOI: 10.1089/neu.2013.2952

Original Articles

Neuroimaging, Behavioral, and Psychological Sequelae of Repetitive Combined Blast/Impact Mild Traumatic Brain Injury in Iraq and Afghanistan War Veterans

Eric C. Petrie,[1–3] Donna J. Cross,[3] Vasily L. Yarnykh,[3] Todd Richards,[3] Nathalie M. Martin,[3] Kathleen Pagulayan,[1,2] David Hoff,[1] Kim Hart,[1] Cynthia Mayer,[1] Matthew Tarabochia,[1] Murray A. Raskind,[1,2] Satoshi Minoshima,[3] and Elaine R. Peskind[1,2]

Abstract

Whether persisting cognitive complaints and postconcussive symptoms (PCS) reported by Iraq and Afghanistan war veterans with blast- and/or combined blast/impact-related mild traumatic brain injuries (mTBIs) are associated with enduring structural and/or functional brain abnormalities versus comorbid depression or posttraumatic stress disorder (PTSD) remains unclear. We sought to characterize relationships among these variables in a convenience sample of Iraq and Afghanistan-deployed veterans with ($n = 34$) and without ($n = 18$) a history of one or more combined blast/impact-related mTBIs. Participants underwent magnetic resonance imaging of fractional anisotropy (FA) and macromolecular proton fraction (MPF) to assess brain white matter (WM) integrity; [^{18}F]-fluorodeoxyglucose positron emission tomography imaging of cerebral glucose metabolism (CMRglu); structured clinical assessments of blast exposure, psychiatric diagnoses, and PTSD symptoms; neurologic evaluations; and self-report scales of PCS, combat exposure, depression, sleep quality, and alcohol use. Veterans with versus without blast/impact-mTBIs exhibited reduced FA in the corpus callosum; reduced MPF values in subgyral, longitudinal, and cortical/subcortical WM tracts and gray matter (GM)/WM border regions (with a possible threshold effect beginning at 20 blast-mTBIs); reduced CMRglu in parietal, somatosensory, and visual cortices; and higher scores on measures of PCS, PTSD, combat exposure, depression, sleep disturbance, and alcohol use. Neuroimaging metrics did not differ between participants with versus without PTSD. Iraq and Afghanistan veterans with one or more blast-related mTBIs exhibit abnormalities of brain WM structural integrity and macromolecular organization and CMRglu that are not related to comorbid PTSD. These findings are congruent with recent neuropathological evidence of chronic brain injury in this cohort of veterans.

Key words: diffusion tensor imaging; macromolecular proton fraction; mild traumatic brain injury; positron emission tomography; veterans

Introduction

As a result of the widespread use of improvised explosive devices against United States (US) military personnel deployed to the conflicts in Iraq and Afghanistan, large numbers of active duty service members and combat veterans have sustained one or more blast- and/or combined blast/impact-related mild traumatic brain injuries (mTBIs) as defined by American Congress of Rehabilitation Medicine (ACRM) criteria.[1] Many of these persons report persisting cognitive complaints (e.g., poor concentration, slowed thinking, short-term memory impairment) and/or other post-concussive symptoms (PCS, e.g., headache, sleep disruption, daytime fatigue, irritability) years after blast/impact-mTBI. Whether these chronic symptoms are accompanied by detectable alterations in brain structure and/or function has been unclear. Recent reports that hyperphosphorylated tau neurofibrillary tangles (NFTs) characteristic of chronic traumatic encephalopathy (CTE) have been observed *postmortem* in the brains of 26 Iraq and Afghanistan veterans with *antemortem* repetitive mTBI[2–4] lend urgency to answering this question.

Several investigators have used magnetic resonance (MR) diffusion tensor imaging (DTI) to interrogate brain white matter (WM) integrity in veterans with and without blast/impact mTBI exposure.[5–9] Findings to date have been inconsistent, however. We

[1]Veterans Affairs (VA) Northwest Network (VISN 20) Mental Illness, Research, Education, and Clinical Center (MIRECC), VA Puget Sound, Seattle, Washington.
[2]Department of Psychiatry and Behavioral Sciences, University of Washington, Seattle, Washington.
[3]Department of Radiology, University of Washington, Seattle, Washington.

previously reported [^{18}F]-fluorodeoxyglucose positron emission tomography ([^{18}F]FDG-PET) imaging evidence of corticocerebellar hypometabolism in a small group of Iraq and Afghanistan veterans with blast-mTBI.[10] The control group consisted of civilians without history of military service, however, raising the possibility that unmeasured behavioral and/or environmental variables associated with military enlistment, training, and/or deployment, rather than blast exposure *per se*, may have influenced the results.

To address this issue, we performed [^{18}F]FDG-PET imaging of regional cerebral glucose metabolism (CMRglu) in Iraq and Afghanistan deployed veterans with (blast-mTBI veterans) and without (nonblast veterans) one or more blast and/or combined blast/impact-related mTBIs. To assess CMRglu associations with WM integrity and to allow comparison with other studies of blast-exposed veterans, we also performed DTI measurements of fractional anisotropy (FA), a metric of WM structural integrity, and macromolecular proton fraction (MPF) mapping,[11–14] a new quantitative metric of WM myelin compositional integrity based on the magnetization transfer effect.[11,15–17] To estimate the possible contribution of comorbid posttraumatic stress disorder (PTSD) to brain abnormalities in blast-mTBI veterans, we compared neuroimaging findings between blast-mTBI veterans with and without a diagnosis of PTSD.

Methods

Participants

The Veterans Affairs (VA) Puget Sound Health Care System and University of Washington Institutional Review Boards approved all procedures, and all participants provided written informed consent before study enrollment. The study participants were a convenience sample recruited from veterans seeking health care from VA Puget Sound. Study staff prescreened VA medical records of Iraq and/or Afghanistan veterans, both with and without mTBI, who were patients in the Deployment Health, PTSD, general Mental Health, and Dental clinics, to identify veterans potentially eligible for study participation, who were then referred by their VA providers to study staff. In addition, veterans were recruited via flyers and advertisements posted within VA Puget Sound and at area universities, community colleges, gyms, and cafes; via Craig's list postings; via presentations at Deployment Health, PTSD, and general Mental Health Clinic staff meetings by ERP; and via word-of-mouth by study participants.

All participants had been deployed to Iraq and/or Afghanistan with the US Armed Forces. The 34 male blast-mTBI veterans were 31.6 ± 9.2 (mean $\pm$ standard deviation [SD]) years of age (range 23–60 years) and had 13.7 ± 1.5 years of education, and the 18 nonblast veterans (17 males, 1 female) were 32.8 ± 7.3 (range 22–46) years of age and reported 14.1 ± 1.5 years of education. The groups did not differ with respect to age or to education ($p > 0.05$). To meet inclusion criteria, all blast-mTBI veterans had to have experienced at least one war zone blast or combined blast/impact exposure that resulted in acute mTBI as defined by ACRM criteria[1] (modified to exclude Glasgow Coma Scale scores, which were not available in the combat setting). The nonblast veterans reported no lifetime history of mTBI by ACRM criteria (except one who was briefly dazed and confused after an impact head injury at age 16).

None of the participants had a history of head injury with loss of consciousness (LOC) exceeding 30 min (i.e., the maximum duration of LOC specified in the ACRM criteria for mTBI); penetrating head wound; seizure disorder; insulin dependent diabetes; current or past *Diagnostic and Statistical Manual of Mental Disorders-IV (DSM-IV)* diagnoses of schizophrenia, other psychotic disorders, bipolar disorder, dementia; or an alcohol or other substance abuse diagnosis within the previous 3 months. Participants using medications potentially affecting brain function, such as opioids, benzodiazepines, or sedating antihistamines, were asked not to take those medications for 24 h before [^{18}F]FDG-PET imaging. Participants with retained shrapnel; ferromagnetic medical implants or prostheses; foreign metal objects; with metal fragments in the eyes (ruled out by computed tomography radiography of the orbits if suspected by history); and/or tattooed eyeliner or other facial tattoos were excluded from MR imaging studies but were not excluded from participation in other study procedures.

mTBI assessments in blast-mTBI veterans

Blast exposure and mTBI histories were obtained from blast-mTBI veterans during a semi-structured interview in which specific inquiries were made regarding total number of blast exposures accompanied by acute symptoms of mTBI (both in Iraq/Afghanistan and in other military and nonmilitary settings) and lifetime TBI history. This interview was designed by the authors in collaboration with three former senior noncommissioned officers who served in a Army Stryker brigade in Mosul, Iraq, in 2004–2005 (see Acknowledgements). No previously published TBI assessment instrument or interview format was used.

Our instrument, the Quantification of Cumulative Blast Exposure (QCuBE), queried lifetime history of any TBI; number of mTBIs (separated into those with and without LOC less than 30 min) associated with blast exposure and, separately, with blunt head trauma, both during deployment to Iraq/Afghanistan and also during participants' entire period of military service; number of mTBIs resulting in evaluation by a medic or at a field hospital, evacuation to another medical facility, temporary light duty restriction, and temporary or permanent reassignment. In addition, the number of acute PCS occurring at the time of what participants described as their most severe blast exposures (up to five per participant) were recorded in detail. These included: LOC (and duration, if LOC occurred); dazed; confused; disoriented; time seemed slowed; events felt unreal or dreamlike; saw stars/''bell rung''; amnesia/memory loss; vision loss/blinded; blurry vision; double vision; tunnel vision; ringing ears; hearing muffled/lost; bleeding from ears; dizziness, vertigo (world spinning); unsteady on feet; nausea; vomiting; headache; none; and other. A printed list of these acute PCS was provided to participants during the QCuBE interview to ensure uniformity of symptom queries. The QCuBE was performed by ERP, ECP, CLM, DJH, KLH, in pairs. All did pairwise cross-training with each other to establish a consensus criterion for each item response.

Behavioral assessments

The Structured Clinical Interview for *DSM-IV*[18] was used to establish diagnoses of Axis I psychiatric disorders. The Clinician Administered PTSD Scale (CAPS)[19,20] was used to establish PTSD diagnoses and to quantify PTSD symptoms. Participants also rated lifetime combat exposure on the Combat Experiences Scale (CES),[21] current PTSD symptom severity on the PTSD Checklist-Military version (PCL-M),[22] symptoms of depression on the Patient Health Questionnaire-9 (PHQ-9),[23] sleep disturbance on the Pittsburgh Sleep Quality Index (PSQI),[24] alcohol use on the Alcohol Use Disorders Identification Test-Consumption Questions (AUDIT-C),[25] and current post-concussive symptoms on the Neurobehavioral Symptom Inventory (NSI).[26]

Neurological assessments

Because parkinsonian motor signs have been observed in patients with repetitive mTBI and CTE,[27] all participants underwent a full neurological examination, including the Unified Parkinson's Disease Rating Scale (UPDRS) motor section.[28] Olfactory function was assessed using the Brief Smell Identification Test.[29]

[^{18}F]FDG-PET image acquisition and pre-processing

Brain [^{18}F]FDG-PET images were acquired on a GE Advance scanner (GE Medical Systems, Milwaukee, WI; axial resolution 4.25 mm full-width-half-maximum [FWHM] at the center), after intravenous infusion of 8–10 mCi of [^{18}F]-FDG. Because our previous work[10] demonstrated that blast-exposed participants would likely have sustained injuries to many of the brain structures typically used as physiologically intact ''reference'' regions for voxel-intensity normalization (such as the cerebellum and the pons), voxel intensities were normalized to mean whole brain CMRglu, which also adjusted for scan-to-scan differences in [^{18}F]FDG specific activity, injected dose, and effects of blood glucose levels on brain uptake.

Automated coregistration; voxel-intensity normalization; spatial normalization (linear size adjustment and nonlinear warping) to a T-1-based [^{18}F]FDG-PET brain atlas in Talairach stereotactic coordinate space;[30] image smoothing using a 2.25 mm^3 Gaussian kernel (approximately one-half the PET scanner FWHM axial resolution); peak cortical and subcortical CMRglu extraction and surface projection; and generation of stereotactically defined volumes-of-Interest (VOIs) were performed with Neurostat/3D-SSP.[31–35] Pre-defined VOIs were generated for right and left frontal, medial frontal, parietal, medial parietal, temporal, medial temporal, anterior cingulate, posterior cingulate, somatosensory, and visual cortices; right and left thalami, cerebellar hemispheres, and vermi; and the pons. In addition, 4.5 mm (i.e., two voxel) diameter spherical VOIs centered at the Talairach atlas coordinates of between-group differences identified on voxelwise whole-brain analyses were generated to estimate the magnitude of between group differences in imaging parameters.

DTI and MPF image acquisition

Brain FA and source images for MPF mapping were acquired on a 3.0 T Philips Achieva whole body scanner (Philips Medical Systems, Best, Netherlands) with a transmit-receive head coil. The FA image acquisition protocol used a single-shot spin-echo echo-planar imaging sequence with TR = 10.56 sec; TE = 60 msec; flip angle = 80 degrees; matrix size = 128 × 128; field of view (FOV) = 240 × 240; slice thickness = 3 mm; 32 gradient directions; and *b*-factors = 0 and 1,000s/mm^2. The MPF image acquisition protocol was modified from that of Yarnykh,[14] to improve spatial resolution, and consisted of: (a) a MT-weighted spoiled three-dimensional (3D) gradient-echo (GRE) sequence (TR/TE = 43/2.3 msec, flip angle = 10 degrees) with an off-resonance saturation pulse (offset frequency = 4 kHz, saturation flip angle = 950 degrees, duration = 19 msec); (b) a reference 3D GRE sequence with the same imaging parameters and without saturation; (c) three 3D GRE sequences for T1-relaxation-time mapping, using variable flip angles (TR/TE = 20/2.3 msec, flip angles = 3, 10, and 20 degrees), and an optimized spoiling scheme;[36] (d) a 3D B0 mapping sequence (TR/TE1/TE2 = 20/2.3/3.3ms, flip angle = 10 degrees) based on the dual-echo GRE phase-difference method;[37] and (e) a 3D actual flip angle B1 mapping sequence (TR1/TR2/TE = 25/125/2.3 msec, flip angle = 60 degrees).[36,38]

Actual spatial resolution was 1.5 × 1.5 × 3.0 mm^3 (3D matrix size = 160 × 120 × 60, FOV = 24 × 18 × 18 cm) for all images except for field maps. B0 and B1 maps were acquired with resolution of 2 × 3 × 3 mm^3 and 2 × 3 × 6 mm^3, respectively. All raw data were zero-interpolated to reconstruct 120 slices with 1.5 mm thickness and 1.0 × 1.0 mm^2 in-plane resolution. Voxel intensity normalization was not performed for brain FA and MPF images because both FA and MPF are quantitative values reflecting intrinsic physical properties of brain tissue, with magnitudes directly proportional to the signal acquired by the MR scanner.

Diffusion tensor image pre-processing

DTI head motion, eddy current, and B0-field inhomogeneity-induced geometric distortion corrections were performed using the Oxford FMRI Software Library (FSL) DTI toolbox.[39] DTIPrep[40] was then used to identify and remove image slices with large within-slice intensity differences, wrapping abnormalities, or other artifacts. Participants' FA maps were spatially normalized to Talairach atlas space using Neurostat, because its normalization algorithms are not dependent on imaging modality and have been shown by others to perform comparably to statistical parametric mapping (SPM; The Wellcome Department of Neurology, London, UK) when applied to MR images.[41]

MPF image pre-processing

MPF parametric maps were reconstructed using a two-step voxelwise algorithm. During the first step, the fit of the Ernst equation to variable flip angle data with B1 correction[38] was performed to obtain T1 and proton density (PD) maps. During the second step, the pulsed magnetization transfer matrix equation[13,42] was iteratively solved by the Gauss-Newton method with B0 and B1 correction and standardized constraints for nonadjustable two-pool model parameters[14] to yield MPF maps. The second step of reconstruction was performed only on voxels containing a non-negligible contribution from the brain parenchyma, which was masked by removing nonbrain tissues and cerebrospinal fluid (CSF).

Brain masks were created from PD maps using the FSL Brain Extraction Tool.[43] In addition, CSF was segmented out before reconstruction of MPF maps, because MPF has a zero value in CSF that cannot be reliably determined by the MPF computation algorithm. CSF segmentation was performed using B1-corrected T1 maps by excluding voxels with T1 relaxation times above a threshold value of T1 = 3000 ms.

MPF maps were then single-channel segmented in native space into four tissue classes using the FSL standard automated segmentation tool, FAST[43] using a Markov random field weighting parameter of 0.25, an empirical value found to provide optimal visual smoothness and anatomic consistency. The four tissue classes are: WM; low myelin content GM (lmGM, mainly cortical GM and the caudate nucleus); high myelin content GM (hmGM, mainly the thalamic nuclei [44] and WM/GM border zones); and a superficial layer of gray matter (sGM, that portion of lmGM susceptible to partial volume averaging with CSF) used primarily for suppression of volume averaging effects but not for data analyses. Participants' MPF maps were spatially normalized to Talairach atlas space using Neurostat.

Data analysis

Whole brain voxelwise comparisons of CMRglu, FA, and MPF values in nonblast versus blast-mTBI veterans were performed using *t* statistics, which were then converted to Z scores by means of a probability integral transformation. Statistical significance, controlling the overall Type I error rate at $p = 0.05$ (corresponding Z score of approximately 4.0) for multiple comparisons, was determined using a random Gaussian fields approach.[45] Between group comparisons of mean whole-brain MPF WM, lmGM, hmGM, and sGM values and of nonimaging data were performed using directional (one-tailed) independent groups *t*-statistics (significance level $p < 0.05$), based on *a priori* hypotheses of abnormal imaging metrics, psychological symptoms, and neurological symptoms and signs in blast-mTBI versus nonblast veterans.

To investigate possible threshold or dose-effect relationships between blast-related mTBIs and alterations in brain neuroimaging parameters, additional whole-brain voxelwise analyses were performed comparing MPF and CMRglu values in nonblast veterans with each of three approximately equal-sized subgroups composed of blast-mTBI veterans with military career totals of, respectively, 1–5, 6–19, and 20–100 blast-related mTBIs (similar analyses of FA values could not be performed, because of insufficient FA

image sets to create blast-exposure subgroups large enough for statistical evaluation).

Results

mTBI assessments in blast-mTBI veterans

Blast-mTBI veterans experienced 13.2 ± 16.8 (range 1–66) blast-mTBI events while deployed to Iraq or Afghanistan and a total of 19.6 ± 26.0 blast mTBI events during their entire period of military service. Total military blast-mTBI exposures ranged from 1 to 100, distributed as follows: 1 (9%), 2–5 (29.4%), 6–10 (20.6%), 11–15 (6%), 16–20 (14.7%). 21–50 (9%), and 51–100 (11.8%). Blast-mTBI veterans experienced 1.0 ± 1.1 (range 0–4) blast exposures accompanied by LOC, all of which occurred in Iraq or Afghanistan. Lifetime episodes of head trauma with LOC from any cause were 2.1 ± 2.2 (range 0–11), indicating that approximately 50% of lifetime LOC episodes were associated with military blast exposure. Mean time between last blast-mTBI and study enrollment was 3.8 ± 1.5 (range 1.2–7.1) years.

The 34 blast-mTBI veterans provided information on the 20 QCuBE-assessed acute PCS for a total of 140 of their self-described ''most severe'' blast exposures. They reported experiencing 7.6 ± 3.6 (median = 7; range 1–16) acute PCS per blast-mTBI event. Relative frequencies of acute PCS were: dazed (72%); confused (51%); disoriented (64%); time seemed slowed (58%); events felt unreal or dreamlike (53%); saw stars/''bell rung'' (56%); amnesia/memory loss (16%); vision loss/blinded (12%); blurry vision (26%); double vision (5%); tunnel vision (11%); ringing ears (84%); hearing muffled/lost (70%); bleeding from ears (1%); dizziness (36%), vertigo (world spinning) (19%); unsteady on feet/balance problems (41%); nausea (15%); vomiting (3%); and headache (63%).

Sixteen blast-mTBI veterans reported having been evaluated in the field by a medic for acute PCS after a blast exposure; seven reported having been evaluated in a field hospital; one reported being medically evacuated to other than a field hospital; six reported being temporarily assigned to light duty; and one reported being permanently reassigned after a blast-mTBI event.

Behavioral assessments

Compared with nonblast veterans, the blast-mTBI veterans endorsed more frequent and severe PCS on the NSI; more severe combat exposure on the CES; and had higher PTSD symptom scores on the CAPS and the PCL-M; higher depression scores on the PHQ-9; greater sleep impairment on the PSQI; and greater alcohol use on the AUDIT-C (although no participants in either group met criteria for alcohol abuse or dependence, as noted in the Methods section) (Table 1).

Among the blast-mTBI veterans, higher NSI scores were associated with greater numbers of both Iraq/Afghanistan deployment and total military career blast-related LOCs ($r = 0.347$, $p < 0.05$ for both), but not with number of blast-related mTBIs. As would be expected in this cohort, higher combat exposure scores on the CES were associated with larger numbers of both Iraq/Afghanistan deployment blast mTBIs and blast-related LOCs ($r = 0.433$, $p < 0.01$ and $r = 0.337$, $p < 0.05$, respectively) and total military career blast-mTBIs and blast-related LOCs ($r = 0.318$, $p < 0.05$) for both. No significant associations were found between number of Iraq/Afghanistan or total military blast-mTBIs and scores on the PCL, CAPS, PSQI, PHQ-9, Audit-C, Smell Test, or UPDRS motor section after applying corrections for multiple comparisons. Veterans with more versus fewer than 20 blast-mTBIs had higher CES scores (15.1 ± 1.8 vs. 12.5 ± 2.6, $p < 0.05$), but the groups did not differ with respect to any of the other behavioral assessment measures.

Table 1. Behavioral Assessment Scores: Blast-mTBI Veterans and Nonblast Veterans

Measure	*Blast-mTBI veterans*	*Nonblast veterans*
CAPS	53.8 ± 31.6 (n = 31)	9.1 ± 17.5 (n = 17)[a]
PCL-M	49.5 ± 17.9 (n = 33)	20.7 ± 6.8 (n = 18)[a]
PHQ-9	9.6 ± 7.4 (n = 34)	2.6 ± 3.6 (n = 18)[a]
PSQI	9.4 ± 4.9 (n = 33)	4.3 ± 3.3 (n = 16)[a]
AUDIT-C	4.7 ± 2.4 (n = 34)	3.0 ± 1.7 (n = 18)[b]
NSI	29.5 ± 17.5 (n = 34)	6.5 ± 10.0 (n = 17)[a]
CES	13.3 ± 2.6 (n = 34)	4.0 ± 4.0 (n = 15)[a]

Data are shown as mean ± standard deviation.
[a]$p < 0.001$, [b]$p < 0.01$ (independent groups *t*-test, one-tailed).
CAPS, Clinician Administered posttraumatic stress disorder (PTSD) Scale; PCL-M, PTSD Checklist–Military Version; PHQ-9, Patient Health Questionnaire–9; PSQI, Pittsburgh Sleep Quality Index; AUDIT-C, Alcohol Use Disorders Identification Test–Consumption Questions; NSI, Neurobehavioral Symptom Inventory; CES, Combat Experiences Scale.

With respect to possible overlapping symptoms of PCS and PTSD, we found that the 22 PCS on the NSI that were more frequently rated as moderate, severe, or very severe by blast-mTBI versus nonblast veterans (Table 2) included only five that are described as symptom criteria for PTSD in *DSM-IV* or listed as PTSD symptoms in the CAPS (i.e., feeling anxious/tense, irritability, difficulty falling/staying asleep, poor concentration/attention, and

Table 2. Percent of Blast-mTBI Veterans and Nonblast Veterans Who Rated Neurobehavioral Symptom Inventory Items as Moderate, Severe, or Very Severe

NSI item	*Blast-mTBI veterans (n = 34)*	*Nonblast veterans (n = 17)*
Forgetfulness	68	24*
Feeling anxious/tense[a]	65	12*
Headaches	62	6*
Irritability[a]	62	18*
Difficulty falling/staying asleep[a]	62	12*
Sensitivity to noise	59	0*
Poor concentration/attention[a]	53	18**
Slowed thinking	53	12*
Hearing difficulty	50	0*
Poor frustration tolerance[a]	47	6**
Feeling depressed/sad	44	12**
Fatigue/loss of energy	41	6*
Difficulty making decisions	38	18**
Numbness/tingling on body	35	12**
Sensitivity to light	35	6**
Loss or increase in appetite	32	0**
Poor coordination	21	6**
Loss of balance	21	0**
Vision problems	21	0***
Feeling dizzy	15	6**
Change in taste or smell	15	0***
Nausea	12	0***

[a]Symptom that may also occur in posttraumatic stress disorder (PTSD).
*$p < 0.001$, **$p < 0.01$, ***$p < 0.05$ (independent groups *t*-test, one-tailed).
NSI, neurobehavioral symptom inventory.

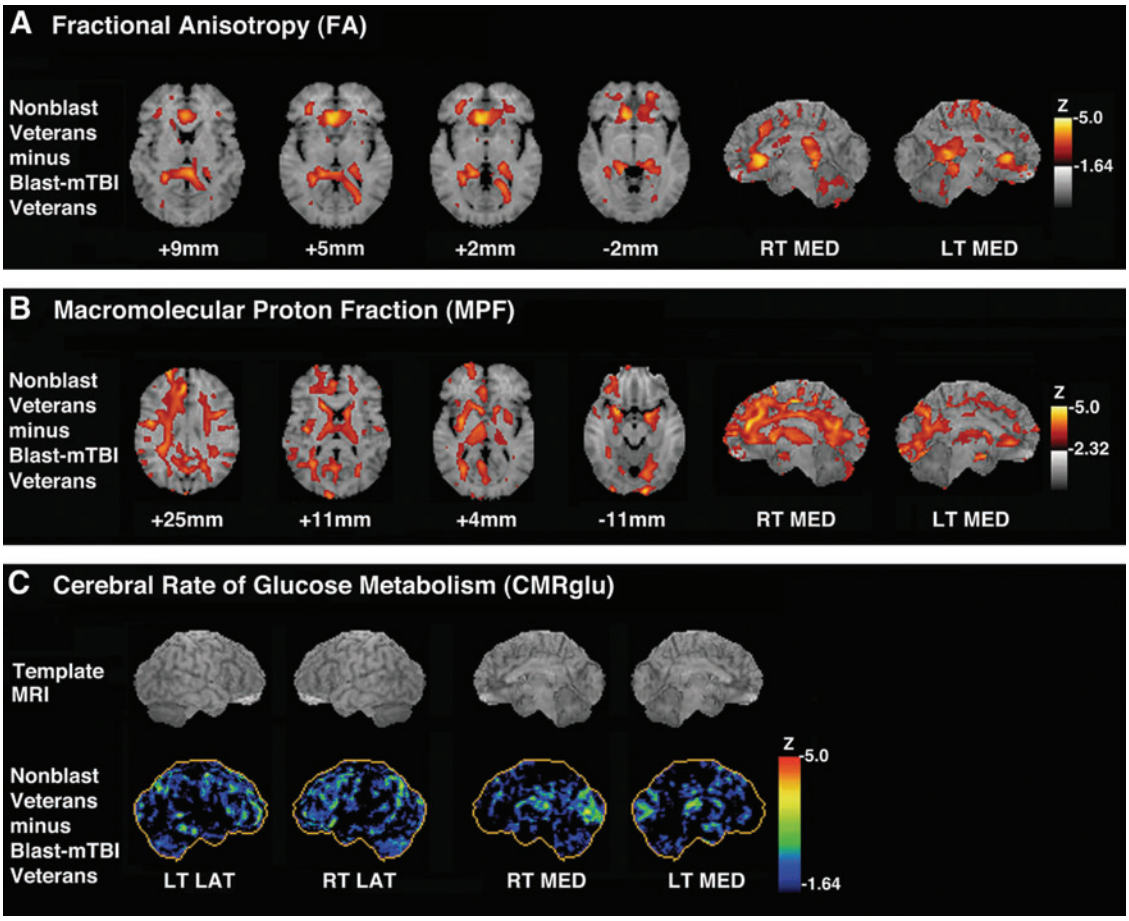

FIG. 1. (**A**) Z-score subtraction maps of fractional anisotropy (FA) values in blast-mild traumatic brain injury (mTBI) veterans (blast mTBI veterans; $n=15$) compared with nonblast veterans ($n=12$), superimposed on magnetic resonance (MR) template images for anatomic orientation (right side of brain is on left side of image). Bar shows color scale versus Z-score, with higher values representing increasing magnitude of FA reduction in blast-mTBI versus nonblast veterans. Shown are horizontal sections through the brain corresponding approximately to Talairach atlas[30] Z-axis coordinates of $+9$ mm, $+5$ mm, $+2$ mm, and -2 mm, as well as views of the right medial (RT MED) and left medial (LT MED) surfaces of the brain. (**B**) Z-score subtraction maps of macromolecular proton fraction (MPF) values in blast-mTBI veterans ($n=27$) compared with nonblast veterans ($n=16$), superimposed on horizontal MR template images for anatomic orientation (right side of brain is on left side of image). Bar shows color scale versus Z-score, with higher values representing increasing magnitude of MPF reduction in blast-mTBI versus nonblast veterans. Shown are horizontal sections through the brain corresponding approximately to Talairach atlas[30] Z-axis coordinates of $+25$ mm, $+11$ mm, $+4$ mm, and -11 mm, as well as views of the right medial (RT MED) and left medial (LT MED) surfaces of the brain. (**C**) Z-score subtraction maps of cerebral rate of glucose metabolism (CMRglu) in blast-mTBI veterans ($n=33$) compared with nonblast veterans ($n=16$). Upper row shows brain MR imaging templates for anatomic orientation. Bar shows color scale versus Z-score, with higher values representing increasing magnitude of hypometabolism in blast-mTBI versus nonblast veteran group. Views are right lateral (RT LAT), left lateral (LT LAT), right medial (RT MED), and left medial (LT MED) surfaces of the brain.

poor frustration tolerance). When the NSI was scored without including these five items, the total score was still greater in blast-mTBI compared with nonblast veterans (20.47 ± 12.8 [$n=34$] vs. 4.12 ± 6.67 [$n=17$], $p<0.001$).

Neurological assessments, UPDRS, Smell Test

None of the participants exhibited focal neurological deficits. Total scores on the UPDRS motor section, however, were higher in blast-mTBI versus nonblast veterans (2.0 ± 2.8 [range 0–9, $n=34$] versus 0.6 ± 1.5 [range 0–6, $n=18$], $p<0.05$). In contrast, scores on the Smell Test did not differ between groups ($p>0.05$).

MR DTI

Whole-brain voxelwise analyses demonstrated reduced FA values in blast-mTBI versus nonblast veterans at two locations within the right genu of the corpus callosum. The VOIs centered at those locations showed FA reductions of 20.7% and 28.1%, respectively (Fig. 1A, 2A).

MPF mapping

Mean whole brain MPF values were lower in blast-mTBI versus nonblast veterans (Fig. 3B) in WM ($13.22\pm0.70\%$ vs. $13.82\pm0.41\%$, $p=0.0017$), hmGM ($8.90\pm0.42\%$ vs. $9.32\pm0.20\%$, $p=0.0003$), and lmGM ($5.78\pm0.26\%$ vs. $6.01\pm0.16\%$, $p=0.0015$), but did not differ with respect to the sGM partial volume component ($3.02\pm0.25\%$ vs. $3.02\pm0.44\%$, $p=0.49$).

Whole-brain voxelwise analyses demonstrated that MPF values were lower in blast-mTBI versus nonblast veterans in multiple brain regions (Fig. 1B, 2B, and Table 3), including cortical-subcortical WM tracts (i.e., right external capsule and right internal

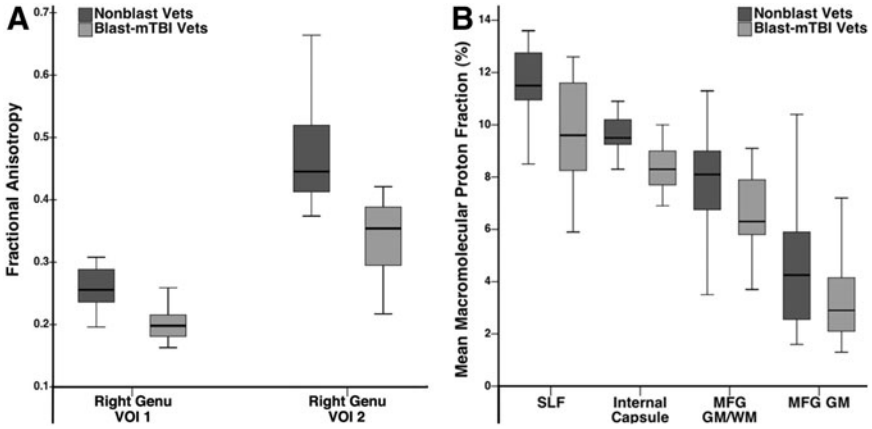

FIG. 2. (**A**) Box and whisker plots showing maximum, third quartile, median, first quartile, and minimum fractional anisotropy values for corpus callosum right genu volumes of interest (VOIs) (centered at atlas coordinates of groupwise differences identified by voxelwise analyses) in 15 blast-mild traumatic brain injury (mTBI) veterans (Blast-mTBI Vets, light gray bars) and 12 nonblast veterans (Nonblast Vets, dark gray bars). (**B**) Box and whisker plots showing maximum, third quartile, median, first quartile, and minimum macromolecular proton fraction values in right superior longitudinal fasciculus (SLF), right internal capsule, anterior limb (internal capsule), right middle frontal gyrus gray matter/white matter border (MFG GM/WM), and right middle frontal gyrus gray matter (MFG GM) VOIs (centered at atlas coordinates of groupwise differences identified by voxelwise analyses) in 27 blast-mTBI veterans (Blast-mTBI Vets, light gray bars) and 16 nonblast veterans (Nonblast Vets, dark gray bars).

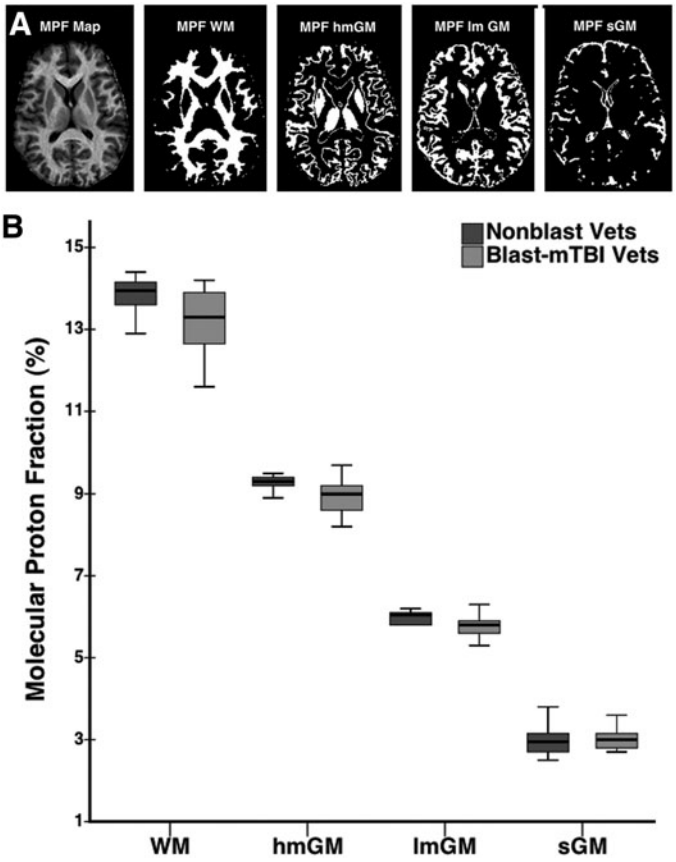

FIG. 3. (**A**) Example segmentation of a molecular proton fraction (MPF) map of a representative participant's brain showing unsegmented MPF map and binary segmentation masks corresponding to white matter (MPF WM), high myelin gray matter (MPF hmGM), low myelin gray matter (MPF lmGM), and superficial gray matter (MPF sGM). (**B**) Box and whisker plots showing maximum, third quartile, median, first quartile, and minimum whole brain MPF WM, hmGM, lmGM, and sGM values for 27 blast-mild traumatic brain injury (mTBI) veterans (Blast-mTBI Vets, light gray bars) compared with 16 nonblast veterans (Nonblast Vets, dark gray bars).

Table 3. Brain Locations of Lower Macromolecular Proton Fraction in Blast-mTBI Veterans ($N=27$) vs. Nonblast Veterans ($N=16$)

Structure[a]	*Tissue*[b]	*Coordinates (mm)*[c]	*Z-score*[d]	*% Reduction*[e]
R external capsule	WM	(−30, −1, 0)	4.4	10.5
R internal capsule, anterior limb	WM	(−17, 17, 9)	4.0	12.3
R superior longitudinal fasciculus	WM	(−44, −6, 27)	4.1	16.3
R superior frontal gyrus	GM	(−24, 59, 22)	4.6	35.8
	WM	(−17, −13, 45)	4.4	7.2
	GM/WM	(−17, 8, 58)	4.0	27.0
	GM/WM	(−6, 32, 27)	4.0	17.6
	GM	(−24, 66, 7)	4.0	36.4
R middle frontal gyrus	WM	(−39, 1, 47)	4.4	19.6
	GM	(−46, 50, −2)	4.1	28.1
	GM/WM	(−37, 48, −4)	4.3	16.7
L inferior frontal gyrus	GM/WM	(42, 5, 20)	4.3	24.3
R medial orbital gyrus	GM	(−26, 37, −16)	4.2	30.5
	GM	(−21, 5, −11)	4.1	18.4
R precentral gyrus	WM	(−19, −17, 45)	4.4	8.1
	GM	(−46, −13, 43)	4.1	19.6
R anterior cingulate gyrus	GM	(−3, 41, 18)	4.5	23.6
L subcallosal gyrus	GM	(15, 3, −14)	4.3	32.5
L superior parietal lobule	WM	(15, −62, 32)	4.0	15.6
R precuneus	WM	(−21, −58, 38)	4.2	16.8
L lingual gyrus	GM	(12, −91, −11)	4.2	20.2

[a]Assigned with reference to Talairach and Tournoux[30] and John's Hopkins University[71] brain atlases. R, right; L, left.
[b]GM, gray matter; WM, white matter; GM/WM, gray matter/white matter border region.
[c]Talairach atlas coordinates of significant between-group differences in MPF by whole brain voxel-wise analyses. For x-axis, positive values are left of midline and negative values are right of midline. For z-axis, positive values are superior to plane of line connecting anterior and posterior commissures. For y-axis, positive and negative values are anterior versus posterior (respectively) of the anterior commissure.
[d]Z-score resulting from probability integral transformation of *t*-statistic for between-group comparison at voxel coordinates given in column 3.
[e]Percent reduction (blast-mTBI vs. nonblast veterans) in mean MPF values for 4.5 mm diameter volumes-of-interest centered on Talairach atlas coordinates of significant (i.e., $Z \geq 4.0$) voxel-wise between group differences.

capsule-anterior limb); the interlobar right superior longitudinal fasciculus; frontal and parietal subgyral WM (i.e., right precentral, superior and middle frontal gyri, medial parietal gyrus/precuneus, and left superior parietal lobule); frontal GM/WM border regions (i.e., right superior and middle frontal and left inferior frontal gyri); and multiple cortical GM regions (i.e., right superior and middle frontal, precentral, and anterior cingulate and left lingual and subcallosal gyri). VOIs centered on the atlas coordinates of these between-group differences showed that MPF reductions in blast-mTBI versus nonblast veterans ranged between 6.8 and 24.7% in magnitude.

Additional whole-brain voxelwise analyses showed that MPF values were lower in blast-mTBI veterans with more versus fewer than 20 total military blast-related mTBIs at more atlas coordinates distributed among a larger number of brain regions (Table 4). In addition, reduced MPF values in commissural, interlobar, and cortical-subcortical WM tracts and in GM/WM border regions were present only in veterans with greater than 20 total military blast-mTBIs.

[^{18}F]FDG-PET brain imaging

Whole-brain voxelwise analyses showed that, compared with nonblast veterans, blast-mTBI veterans exhibited CMRglu reductions (Z scores ≥ 4.0) in the right and left parietal cortices (1.62% and 1.71%, respectively, based on VOIs); the left somatosensory cortex (1.66% by VOI); and the right visual cortex (3.43% by VOI) (Fig. 1C). Additional whole-brain voxelwise comparisons showed that CMRglu values were lower in veterans with more versus fewer than 20 total military blast-mTBIs at a single atlas coordinate located within the parahippocampal gyrus.

Effects of comorbid PTSD on CMRglu, FA, and MPF

Whole-brain voxelwise analyses indicated that blast-mTBI veterans with versus without PTSD did not differ with respect to CMRglu, FA, or MPF values in any brain regions.

Relationships between neuroimaging measures and behavioral and neurological assessments

Within the blast-mTBI Veteran group, VOI-based correlation analyses showed no statistically significant associations (after corrections for multiple comparisons) between FA or MPF values and any of the behavioral or neurological assessment measures. Similarly negative results were obtained for correlation analyses based on CMRglu values in the sensorimotor and visual cortices.

Relationships among neuroimaging measures

Within the blast-mTBI veteran group, VOI-based correlation analyses showed no statistically significant associations (after corrections for multiple comparisons) between FA and MPF, FA and CMRglu, or MPF and CMRglu values, respectively.

Discussion

Our findings provide evidence that chronic alterations in brain WM structure and composition and cortical glucose

Table 4. Brain Locations of Lower Macromolecular Proton Fraction MPF in Blast-Mild Traumatic Brain Injury Veterans with 1–5, 6–19, and 20–100 Blast Exposures, Respectively, Compared with Nonblast Veterans

Veterans with 1–5 blast-mTBIs (n = *10*) *compared with nonblast veterans* (n = *16*)			
Structure[a]	*Tissue*[b]	*Coordinates (mm)*[c]	*Z-score*[d]
R pyramis (cerebellum)	GM	(−19, −64, −27)	4.45
	GM	(−17, −73, −32)	3.99
L middle temporal gyrus	GM	(66, −37, −4)	4.09
R medial frontal gyrus	WM	(−6, 28, 34)	4.28
	GM	(−3, 39, 25)	3.97
R postcentral gyrus	WM	(−15, −35, 47)	3.98
L lingual gyrus	WM	(12, −91, −11)	4.32
R precuneus	WM	(−8, −64, 20)	4.08
R cuneus	GM	(−1, −62, 16)	3.96
Veterans with 6–19 blast-mTBIs (n = *8*) *compared with nonblast veterans* (n = *16*)			
Structure[a]	*Tissue*[b]	*Coordinates (mm)*[c]	*Z-score*[d]
L Precuneus	WM	(12, −64, 34)	3.95
Veterans with 20–100 blast-mTBIs (n = *9*) *compared with nonblast veterans* (n = *16*)			
Structure[a]	*Tissue*[b]	*Coordinates (mm)*[c]	*Z-score*[d]
R superior frontal gyrus	GM/WM	(−21, 57, 22)	4.85
	GM/WM	(−10, 66, 0)	4.07
	GM	(−24, 59, 27)	4.57
	GM	(−15, 66, 20)	4.56
	GM	(−24, 66, 7)	3.98
	WM	(−17, 53, 7)	4.24
	WM	(−17, −10, 45)	4.20
L superior frontal gyrus	GM/WM	(26, 50, 18)	4.08
L inferior frontal gyrus	GM/WM	(39, 5, 20)	4.54
R middle frontal gyrus	GM/WM	(−37, 48, −4)	4.32
	GM/WM	(−42, 41, 14)	4.17
	GM/WM	(−44, 26, 18)	4.04
	GM	(−46, 50, −4)	3.96
	WM	(−28, 50, 20)	4.12
	WM	(−35, 3, 40)	4.10
	WM	(−39, 35, 32)	4.10
R precentral gyrus	WM	(−21, −19, 45)	4.26
L precentral gyrus	WM	(17, −19, 40)	4.08
		(15, −17, 47)	4.06
R postcentral gyrus	WM	(−37, 3, 45)	4.14
L postcentral gyrus	WM	(57, −13, 22)	4.18
		(19, −33, 40)	4.09
R middle temporal gyrus	GM/WM	(−60, −31, −4)	4.13
L superior parietal lobule	WM	(19, −62, 27)	4.54
		(28, −46, 38)	4.20
R cingulate gyrus	GM	(−3, 30, 27)	4.19
L cingulate gyrus	WM	(3, −28, 32)	4.10
R precuneus	WM	(−21, −60, 43)	4.21
	GM	(−1, −64, 18)	3.99
	GM	(−3, −96, 16)	4.19
	GM	(−10, −94, 11)	3.98
R cingulum (hippocampal part)	WM	(−17, −46, 2)	4.06
L cingulum	WM	(3, −15, 32)	4.74
		(15, 14, 36)	3.96
R corpus callosum, tapetum	WM	(−26, −44, 16)	4.15
R corpus callosum, splenium	WM	(−10, −40, 16)	4.10
L superior longitudinal fasciculus	WM	(35, −13, 34)	4.58
R corona radiata, anterior	WM	(−26, 37, −16)	3.95
L corona radiata, superior	WM	(26, 5, 25)	4.09
R internal capsule, anterior limb	WM	(−17, 17, 9)	4.07
		(−17, 14, 16)	3.95
L external capsule	WM	(28, 1, 2)	4.00
R posterior thalamic radiation	WM	(−26, −58, 7)	4.35

mTBI, mild traumatic brain injury.

[a]Assigned with reference to Talairach and Tournoux[30] and John's Hopkins University[71] brain atlases. R, right; L, left.

[b]GM, gray matter; WM, white matter; GM/WM, gray matter/white matter border region.

[c]Talairach atlas coordinates of significant between-group differences in macromolecular proton fraction by whole brain voxel-wise analyses. For x-axis, positive values are left of midline and negative values are right of midline. For z-axis, positive values are superior to plane of line connecting anterior and posterior commissures. For y-axis, positive and negative values are anterior versus posterior (respectively) of the anterior commissure.

[d]Z-score resulting from probability integral transformation of *t*-value for between-group comparison at voxel coordinates given in column 3.

metabolism are present in Iraq and Afghanistan war veterans with one or more blast-mTBIs compared with those without blast exposure; that there may be a threshold effect governing the relationship between blast-mTBIs and abnormal findings on brain MPF imaging; and that CMRglu, FA, and MPF neuroimaging alterations in this cohort of veterans cannot be attributed to comorbid PTSD.

Compared with nonblast veterans, blast-mTBI veterans in our study had lower FA values in the genu of the corpus callosum, a structure commonly affected by impact head traumas producing diffuse axonal injury (DAI).[46,47] In contrast, Levin and associates,[7] using voxelwise, VOI, and tractography analyses, found no differences in brain FA values among groups of Iraq/Afghanistan veterans with no, mild, or moderate blast-mTBI. In another DTI study, Davenport and colleagues[5] reported that blast-exposed veterans exhibited greater numbers of low FA voxels (i.e., ≤ 2 SD below the mean of non–blast-exposed veterans) within several commissural, interlobar, and cortical-subcortical WM fiber tract VOIs, but that mean FA values in the same VOIs did not differ between groups.

Mac Donald and coworkers[8] reported that military personnel evacuated from Iraq or Afghanistan after a combined blast/impact mTBI versus a non-head injury exhibited reduced FA values in the cingulum bundles, middle cerebellar peduncles, and uncinate fasciculi, as well as the right internal capsule and orbitofrontal white matter. Morey and colleagues[9] found that Iraq/Afghanistan veterans with combined blast/impact mTBIs exhibited reduced FA in numerous commissural, cortical/subcortical, and anterior-posterior interlobar WM tracts and brainstem regions compared with those without TBI. Most recently, Jorge and associates[6] reported that 72 veterans with and 21 without blast/impact-mTBI exposure in Iraq or Afghanistan did not differ with respect to FA values using tract based spatial statistics (TBSS).[48] *Post-hoc* analyses, however, showed more clusters of contiguous low-FA voxels (i.e., < 3 SD below the mean of non–blast-exposed subjects) in the blast/impact mTBI Veterans.

Factors accounting for the contradictory findings in previous studies of blast-mTBI in Iraq and Afghanistan veterans remain unclear but may include differences in subject characteristics and/or imaging protocols. For example, time between blast exposure and imaging ranges between a median of 14 days[8] and 9.7 ± 10.8 years.[9] Participants in our and previous studies also differ with respect to both the relative number and severity of both blast and impact mTBI exposures. In addition, the accuracy and reliability of FA measurements are known to be sensitive to the introduction of artifacts during DTI acquisition, prepossessing, spatial normalization, and statistical analysis.[49–51]

Of particular concern are image analysis strategies that rely on pixel intensities as the basis for spatial normalization and then analyze pixel intensity differences as outcome measures; such ''circular'' analyses may result in inflated Type I error rates.[51,52] Neurostat/3D-SSP, however, optimizes spatial normalization of individual subject images to the Talairach atlas space via anatomically based spatial matching algorithms applied at both the global (linear size adjustment) and regional (nonlinear warping) levels,[31–35,53] minimizing the risk of this confound.

Based on these methodological considerations and the fact that previous studies have differed greatly with respect to DTI acquisition and analysis techniques,[5–9] it is plausible that methodological differences may account for much of the variance in findings across studies. In this regard, our use of Neurostat for spatial normalization of participants' brain FA maps represents yet another potential methodological confound. That the Neurostat spatial normalization algorithm is not modality dependent[34] and has been shown by others to perform comparably to SPM when applied to MR images[41] argues against it having a significant effect on our findings. Possible Type I or Type II errors, however, resulting from inaccuracy of spatial registration are always a concern in brain mapping research, even though the algorithms have been tested and used by others.

Another factor possibly contributing to inconsistencies among previous study results may relate to the biomechanics of brain injuries resulting from explosive blast waves, which may create complex patterns of stress and shear forces within the brain parenchyma (particularly at interfaces between tissues of differing density, such as GM/WM junctions),[54] which may predispose to the development of spatially heterogeneous patterns of injury across individuals,[5,6] rendering them difficult to identify via current voxelwise-, VOI-, and tractography-based image analysis methods.

This is the first study to evaluate blast-mTBI effects on brain structure by means of MPF mapping. Between-group differences in MPF values were evident in cortical-subcortical and interlobar WM tracts, in frontal subgyral WM, and in GM/WM border regions known to be vulnerable to DAI in impact TBI.[46,47,55] This pattern of abnormalities was more evident in veterans sustaining more versus less than 20 blast-mTBIs during military service, suggesting a possible threshold effect of repetitive blast-related mTBIs on MPF imaging abnormalities. Whether these imaging abnomalities represent neuropathologic changes in WM myelin composition remains to be determined. Although reduced MPF values in GM/WM border regions is consistent with neuropathological findings in DAI, we cannot rule out a confounding effect of GM/WM partial volume effects. This represents a thorny methodological problem that is not amenable to resolution by tractography-based methods,[48] which typically threshold out the peripheral margins of WM tracts, where both GM/WM damage and partial volume effects occur. Whether alternative approaches, such as cortical surface-based extraction of diffusion data,[56] can disambiguate these effects remains to be determined.

Other studies of MPF mapping in TBI are not available in the literature. However, whole brain voxelwise imaging of the magnetization transfer ratio (MTR), a less specific metric of myelin composition,[11,15–17] have demonstrated reduced whole brain MTR in impact mTBI with persistent PCS.[57] In addition, there is overlap among brain structures exhibiting reduced MPF in our blast-mTBI veterans and reduced MTR in previous studies of civilian patients with mild, moderate, and severe impact TBI.[58–61]

We previously reported evidence of cerebellar, pontine, thalamic, and medial temporal hypometabolism in blast-mTBI veterans compared with civilian controls without a history of military service or TBI.[10] In contrast, this sample of blast-mTBI veterans exhibited hypometabolism restricted to the bilateral parietal, left sensorimotor, and right visual cortices when compared with deployed veterans without blast-related mTBI. Given that regional hypometabolism after severe impact TBI has been shown to improve during the course of recovery,[62] it is significant that our blast-mTBI veterans continue to exhibit residual CMRglu deficits an average of almost 4 years after their last blast exposure.

Whether cognitive complaints and persisting PCS in Iraq/Afghanistan war veterans with a history of blast-mTBI are manifestations of occult brain injury or of comorbid psychiatric conditions, such as PTSD, has been a source of controversy.[63–65] A number of studies have reported brain DTI abnormalities in patients with PTSD.[66] Our blast-mTBI veterans with versus without PTSD, however, did not differ with respect to brain FA, MPF, or CMRglu

values. Overall, these results argue against comorbid PTSD being responsible for CMRglu, FA, and/or MPF abnormalities in veterans with repetitive blast-mTBI.

Limitations of our study include the small sample size and the fact that both the number of blast exposures and the nature and severity of acute blast-related symptoms were dependent on participant recall. In addition, although we obtained detailed histories of isolated impact mTBI exposures in our blast-mTBI veterans, the large number of blast exposures in this group precluded us from obtaining similarly detailed histories of blast exposures that were and were not accompanied by secondary impact mTBIs. Other investigators have also reported difficulties identifying Iraq or Afghanistan deployed veterans not exposed to both blast and impact mTBI.[5,6,8,9] Finding a ''pure'' blast mTBI sample of deployed veterans may not be possible given the high frequency of blunt head trauma during extended combat operations and/or as secondary and tertiary mechanisms of head injury accompanying blast exposure. Elucidating which alterations in brain structure and/or function in veterans with mTBI are uniquely associated with blast versus impact mechanisms of injury may not be possible until such time as quantitative blast-mTBI metrics can be gathered by wearable electronic sensors, as have recently been used in studies of sports related concussions.[67]

We were unable to identify robust associations between neuroimaging metrics and behavioral and neurological assessment measures within the group of blast-mTBI veterans, despite finding significant between-group differences in several of these variables. The reasons for these discrepancies are unclear. It is possible, however, that spatial heterogeneity in the distribution of blast-related brain injuries among individuals, as mentioned earlier,[5,6] may have decreased the power of our image analysis methods to detect such associations. In addition, the pre-specified VOIs applied to our participants' [^{18}F]FDG-PET images were optimized for detecting the effects of neurodegenerative disorders characterized by predictable patterns of disease onset and progression within large, contiguous areas of cerebral cortex.[68,69] It is possible that blast-injury-related changes in CMRglu in smaller clusters of voxels within these VOIs may have not have been detected.

Similarly, the relatively small number of veterans with greater versus less than 20 blast-mTBIs may have resulted in insufficient statistical power to detect associations between numbers of blast-mTBIs and scores on behavioral and neurological assessment measures. Finally, as noted earlier, errors resulting from inaccuracy of spatial registration are always a concern in brain mapping research and cannot be completely ruled out here. Additional research needs to be performed to further confirm our current findings.

To what degree, if any, brain FA, MPF, and/or CMRglu abnormalities in blast-mTBI veterans are associated with abnormalities of tau phosphorylation and/or NFT formation, as recently demonstrated neuropathologically in 26 Iraq/Afghanistan veterans with repetitive mTBI,[2–4] is unknown. Imaging studies of professional boxers,[70] a group at high risk for the development of CTE,[27] have reported decreased FA in many of the same WM tracts as our veterans with blast-mTBI exposure.[5,8,9] Whether changes in WM integrity seen on DTI and MPF and NFTs demonstrated neuropathologically by others[2–4] are causally related or are separate and physiologically distinct outcomes of repetitive mTBI remains to be determined. Longitudinal studies of blast-mTBI veterans combining neuroimaging and CSF neurodegenerative dementia biomarker measurements and sensitive neurocognitive evaluations are needed to clarify the long-term risk for CTE in this cohort of veterans.

Acknowledgments

The authors wish to thank James J. O'Connell, MSW, for performing the SCID and CAPS structured clinical interviews and Command Sgt. MAJ (ret) Thomas Adams, Command Sgt. MAJ (ret) Robert Prosser, and First Sgt. (ret) Creed McCaslin for assistance in constructing the Quantification of Cumulative Blast Exposure (QCuBE) instrument.

This material is based on work supported, in part, by the Department of Veterans Affairs Rehabilitation Research and Development Service (B77421), VA Clinical Science Research and Development CAREER development award TK2 CX000516, and VA Northwest Network MIRECC; National Institute of Health grants AG05136, 5K08AG23670, and R21EB009908; and an anonymous foundation.

Author Disclosure Statement

No competing financial interests exist.

References

1. Kay, T., Harrington, D.E., Adams, R., Anderson, T., Berrol, S., Cicerone, K., Dahlberg, C., Gerber, D., Goka, R., Harley, P., Hilt, J., Horn, L., Lehmkuhl, D., and Malec, J. (1993). Definition of mild traumatic brain injury. J. Head Trauma Rehabil. 8, 86–87.
2. Goldstein, L.E., Fisher, A.M., Tagge, C.A., Zhang, X.L., Velisek, L., Sullivan, J.A., Upreti, C., Kracht, J.M., Ericsson, M., Wojnarowicz, M.W., Goletiani, C.J., Maglakelidze, G.M., Casey, N., Moncaster, J.A., Minaeva, O., Moir, R.D., Nowinski, C.J., Stern, R.A., Cantu, R.C., Geiling, J., Blusztajn, J.K., Wolozin, B.L., Ikezu, T., Stein, T.D., Budson, A.E., Kowall, N.W., Chargin, D., Sharon, A., Saman, S., Hall, G.F., Moss, W.C., Cleveland, R.O., Tanzi, R.E., Stanton, P.K., and McKee, A.C. (2012). Chronic traumatic encephalopathy in blast-exposed military veterans and a blast neurotrauma mouse model. Sci. Transl. Med. 4, 134ra160.
3. McKee, A.C., Stern, R.A., Nowinski, C.J., Stein, T.D., Alvarez, V.E., Daneshvar, D.H., Lee, H.S., Wojtowicz, S.M., Hall, G., Baugh, C.M., Riley, D.O., Kubilus, C.A., Cormier, K.A., Jacobs, M.A., Martin, B.R., Abraham, C.R., Ikezu, T., Reichard, R.R., Wolozin, B.L., Budson, A.E., Goldstein, L.E., Kowall, N.W., and Cantu, R.C. (2013). The spectrum of disease in chronic traumatic encephalopathy. Brain 136, 43–64.
4. Omalu, B., Hammers, J.L., Bailes, J., Hamilton, R.L., Kamboh, M.I., Webster, G., and Fitzsimmons, R.P. (2011). Chronic traumatic encephalopathy in an Iraqi war veteran with posttraumatic stress disorder who committed suicide. Neurosurg. Focus 31, E3.
5. Davenport, N.D., Lim, K.O., Armstrong, M.T., and Sponheim, S.R. (2012). Diffuse and spatially variable white matter disruptions are associated with blast-related mild traumatic brain injury. Neuroimage 59, 2017–2024.
6. Jorge, R.E., Acion, L., White, T., Tordesillas-Gutierrez, D., Pierson, R., Crespo-Facorro, B., and Magnotta, V.A. (2012). White matter abnormalities in veterans with mild traumatic brain injury. Am. J. Psychiatry 169, 1284–1291.
7. Levin, H.S., Wilde, E., Troyanskaya, M., Petersen, N.J., Scheibel, R., Newsome, M., Radaideh, M., Wu, T., Yallampalli, R., Chu, Z., and Li, X. (2010). Diffusion tensor imaging of mild to moderate blast-related traumatic brain injury and its sequelae. J. Neurotrauma 27, 683–694.
8. Mac Donald, C.L., Johnson, A.M., Cooper, D., Nelson, E.C., Werner, N.J., Shimony, J.S., Snyder, A.Z., Raichle, M.E., Witherow, J.R., Fang, R., Flaherty, S.F., and Brody, D.L. (2011). Detection of blast-related traumatic brain injury in U.S. military personnel. N. Engl. J. Med. 364, 2091–2100.
9. Morey, R.A., Haswell, C.C., Selgrade, E.S., Massoglia, D., Liu, C., Weiner, J., Marx, C.E.; MIRECC Work Group, Cernak, I., McCarthy, G. (2013). Effects of chronic mild traumatic brain injury on white matter integrity in Iraq and Afghanistan war Veterans. Hum. Brain Mapp. 34, 2986–2999.
10. Peskind, E.R., Petrie, E.C., Cross, D.J., Pagulayan, K., McCraw, K., Hoff, D., Hart, K., Yu, C.E., Raskind, M.A., Cook, D.G., and

Minoshima, S. (2011). Cerebrocerebellar hypometabolism associated with repetitive blast exposure mild traumatic brain injury in 12 Iraq war Veterans with persistent post-concussive symptoms. Neuroimage 54, S76–S82.
11. Underhill, H.R., Rostomily, R.C., Mikheev, A.M., Yuan, C., and Yarnykh, V.L. (2011). Fast bound pool fraction imaging of the in vivo rat brain: association with myelin content and validation in the C6 glioma model. Neuroimage 54, 2052–2065.
12. Underhill, H.R., Yuan, C., and Yarnykh, V.L. (2009). Direct quantitative comparison between cross-relaxation imaging and diffusion tensor imaging of the human brain at 3.0 T. Neuroimage 47, 1568–1578.
13. Yarnykh, V.L., and Yuan, C. (2004). Cross-relaxation imaging reveals detailed anatomy of white matter fiber tracts in the human brain. Neuroimage 23, 409–424.
14. Yarnykh, V.L. (2012). Fast macromolecular proton fraction mapping from a single off-resonance magnetization transfer measurement. Magn. Reson. Med. 68, 166–178.
15. Rausch, M., Tofts, P., Lervik, P., Walmsley, A., Mir, A., Schubart, A., and Seabrook, T. (2009). Characterization of white matter damage in animal models of multiple sclerosis by magnetization transfer ratio and quantitative mapping of the apparent bound proton fraction f. Mult. Scler. 15, 16–27.
16. Samsonov, A., Alexander, A.L., Mossahebi, P., Wu, Y.C., Duncan, I.D., and Field, A.S. (2012). Quantitative MR imaging of two-pool magnetization transfer model parameters in myelin mutant shaking pup. Neuroimage 62, 1390–1398.
17. Schmierer, K., Tozer, D.J., Scaravilli, F., Altmann, D.R., Barker, G.J., Tofts, P.S., and Miller, D.H. (2007). Quantitative magnetization transfer imaging in postmortem multiple sclerosis brain. J. Magn. Reson. Imaging 26, 41–51.
18. First, M.B., Spitzer, R.L., Gibbon, M. and Williams, J.B. (2002). Structured Clinical Interview for DSM-IV-TR Axis I Disorders, Research Version, Patient Edition. (SCID-I/P). Biometrics Research, New York State Psychiatric Institute: New York.
19. Blake, D.D., Weathers, F.W., Nagy, L.M., Kaloupek, D.G., Gusman, F.D., Charney, D.S., and Keane, T.M. (1995). The development of a Clinician-Administered PTSD Scale. J. Trauma Stress 8, 75–90.
20. Weathers, F.W., Ruscio, A.M., and Keane, T.M. (1999). Psychometric properties of nine scoring rules for the Clinician-Administered Posttraumatic Stress Disorder Scale. Psychol. Assess. 11, 124–133.
21. Killgore, W.D., Cotting, D.I., Thomas, J.L., Cox, A.L., McGurk, D., Vo, A.H., Castro, C.A., and Hoge, C.W. (2008). Post-combat invincibility: violent combat experiences are associated with increased risk-taking propensity following deployment. J. Psychiatr. Res. 42, 1112–1121.
22. Forbes, D., Creamer, M., and Biddle, D. (2001). The validity of the PTSD checklist as a measure of symptomatic change in combat-related PTSD. Behav. Res. Ther. 39, 977–986.
23. Kroenke, K., Spitzer, R.L. and Williams, J.B. (2001). The PHQ-9: validity of a brief depression severity measure. J. Gen. Intern. Med. 16, 606–613.
24. Buysse, D.J., Reynolds, C.F., 3rd, Monk, T.H., Berman, S.R., and Kupfer, D.J. (1989). The Pittsburgh Sleep Quality Index: a new instrument for psychiatric practice and research. Psychiatry Res. 28, 193–213.
25. Bush, K., Kivlahan, D.R., McDonell, M.B., Fihn, S.D., and Bradley, K.A. (1998). The AUDIT alcohol consumption questions (AUDIT-C): an effective brief screening test for problem drinking. Ambulatory Care Quality Improvement Project (ACQUIP). Alcohol Use Disorders Identification Test. Arch. Intern. Med. 158, 1789–1795.
26. Cicerone, K., and Kalmar, K. (1995). Persistent postconcussion syndrome: the structure of subjective complaints after mild traumatic brain injury. J. Head Trauma Rehabil. 10, 1–17.
27. Stern, R.A., Riley, D.O., Daneshvar, D.H., Nowinski, C.J., Cantu, R.C., and McKee, A.C. (2011). Long-term consequences of repetitive brain trauma: chronic traumatic encephalopathy. PM R 3, Suppl 2, S460–S467.
28. Martinez-Martin, P., Gil-Nagel, A., Gracia, L.M., Gomez, J.B., Martinez-Sarries, J., and Bermejo, F. (1994). Unified Parkinson's Disease Rating Scale characteristics and structure. The Cooperative Multicentric Group. Mov. Disord. 9, 76–83.
29. Doty, R.L., Marcus, A., and Lee, W.W. (1996). Development of the 12-item Cross-Cultural Smell Identification Test (CC-SIT). Laryngoscope 106, 353–356.
30. Talairach, J., and Tournoux, P. (1988). *Co-Planar Stereotaxic Atlas of the Human Brain. 3-Dimensional Proportional System: An Approach to Cerebral Imaging*. Thieme Medical Publishers: New York.
31. Minoshima, S., Berger, K.L., Lee, K.S., and Mintun, M.A. (1992). An automated method for rotational correction and centering of three-dimensional functional brain images. J. Nucl. Med. 33, 1579–1585.
32. Minoshima, S., Frey, K.A., Koeppe, R.A., Foster, N.L., and Kuhl, D.E. (1995). A diagnostic approach in Alzheimer's disease using three-dimensional stereotactic surface projections of fluorine-18-FDG PET. J. Nucl. Med. 36, 1238–1248.
33. Minoshima, S., Koeppe, R.A., Frey, K.A., Ishihara, M., and Kuhl, D.E. (1994). Stereotactic PET atlas of the human brain: aid for visual interpretation of functional brain images. J. Nucl. Med. 35, 949–954.
34. Minoshima, S., Koeppe, R.A., Frey, K.A., and Kuhl, D.E. (1994). Anatomic standardization: linear scaling and nonlinear warping of functional brain images. J. Nucl. Med. 35, 1528–1537.
35. Minoshima, S., Koeppe, R.A., Mintun, M.A., Berger, K.L., Taylor, S.F., Frey, K.A., and Kuhl, D.E. (1993). Automated detection of the intercommissural line for stereotactic localization of functional brain images. J. Nucl. Med. 34, 322–329.
36. Yarnykh, V.L. (2010). Optimal radiofrequency and gradient spoiling for improved accuracy of T1 and B1 measurements using fast steady-state techniques. Magn. Reson. Med. 63, 1610–1626.
37. Skinner, T.E., and Glover, G.H. (1997). An extended two-point Dixon algorithm for calculating separate water, fat, and B0 images. Magn. Reson. Med. 37, 628–630.
38. Yarnykh, V.L. (2007). Actual flip-angle imaging in the pulsed steady state: a method for rapid three-dimensional mapping of the transmitted radiofrequency field. Magn. Reson. Med. 57, 192–200.
39. Smith, S.M., Jenkinson, M., Woolrich, M.W., Beckmann, C.F., Behrens, T.E., Johansen-Berg, H., Bannister, P.R., De Luca, M., Drobnjak, I., Flitney, D.E., Niazy, R.K., Saunders, J., Vickers, J., Zhang, Y., De Stefano, N., Brady, J.M., and Matthews, P.M. (2004). Advances in functional and structural MR image analysis and implementation as FSL. Neuroimage 23, Suppl 1, S208–S219.
40. Liu, X., Zhu, H., Marks, B.L., Katz, L.M., Goodlett, C.B., Gerig, G., and Styner, M. (2009). Voxelwise group analysis of DTI. In: *2009 IEEE International Symposium on Biomedical Imaging (ISBI): From Nano to Macro*. Institute of Electrical and Electronics Engineers (IEEE): Boston, MA, pps. 807–810.
41. Hosaka, K., Ishii, K., Sakamoto, S., Sadato, N., Fukuda, H., Kato, T., Sugimura, K., and Senda, M. (2005). Validation of anatomical standardization of FDG PET images of normal brain: comparison of SPM and NEUROSTAT. Eur. J. Nucl. Med. Mol. Imaging 32, 92–97.
42. Yarnykh, V.L. (2002). Pulsed Z-spectroscopic imaging of cross-relaxation parameters in tissues for human MRI: theory and clinical applications. Magn. Reson. Med. 47, 929–939.
43. Smith, S.M. (2002). Fast robust automated brain extraction. Hum. Brain Mapp. 17, 143–155.
44. le Gros Clark, W.E. (1936). The termination of ascending tracts in the thalamus of the macaque monkey. J. Anat. 71, 7–40.
45. Worsley, K.J., Evans, A.C., Marrett, S., and Neelin, P. (1992). A three-dimensional statistical analysis for CBF activation studies in human brain. J. Cereb. Blood Flow Metab. 12, 900–918.
46. Adams, J.H., Doyle, D., Ford, I., Gennarelli, T.A., Graham, D.I., and McLellan, D.R. (1989). Diffuse axonal injury in head injury: definition, diagnosis and grading. Histopathology 15, 49–59.
47. Strich, S.J. (1956). Diffuse degeneration of the cerebral white matter in severe dementia following head injury. J. Neurol. Neurosurg. Psychiatry 19, 163–185.
48. Smith, S.M., Jenkinson, M., Johansen-Berg, H., Rueckert, D., Nichols, T.E., Mackay, C.E., Watkins, K.E., Ciccarelli, O., Cader, M.Z., Matthews, P.M., and Behrens, T.E. (2006). Tract-based spatial statistics: voxelwise analysis of multi-subject diffusion data. Neuroimage 31, 1487–1505.
49. Jones, D.K., and Cercignani, M. (2010). Twenty-five pitfalls in the analysis of diffusion MRI data. NMR Biomed. 23, 803–820.
50. Edden, R.A., and Jones, D.K. (2011). Spatial and orientational heterogeneity in the statistical sensitivity of skeleton-based analyses of diffusion tensor MR imaging data. J. Neurosci. Methods 201, 213–219.
51. Tustison, N.J., Avants, B.B., Cook, P.A., Kim, J., Whyte, J., Gee, J.C. and Stone, J.R. (2012). Logical circularity in voxel-based analysis:

Normalization strategy may induce statistical bias. Hum. Brain Mapp. DOI: 10.1002/hbm.22211. Epub ahead of print
52. Bookstein, F.L. (2001). ''Voxel-based morphometry'' should not be used with imperfectly registered images. Neuroimage 14, 1454–1462.
53. Bookstein, F.L. (1989). Principal warps: thin-plate splines and the decomposition of deformations. IEEE Trans. Pattern Analysis and Machine Intelligence, 11, 567–585.
54. Ling, G., Bandak, F., Armonda, R., Grant, G., and Ecklund, J. (2009). Explosive blast neurotrauma. J. Neurotrauma 26, 815–825.
55. Maxwell, W.L., Povlishock, J.T., and Graham, D.L. (1997). A mechanistic analysis of nondisruptive axonal injury: a review. J. Neurotrauma 14, 419–440.
56. Kang, X., Herron, T.J., Turken, A.U., and Woods, D.L. (2012). Diffusion properties of cortical and pericortical tissue: regional variations, reliability and methodological issues. Magn. Reson. Imaging 30, 1111–1122.
57. Hofman, P.A., Verhey, F.R., Wilmink, J.T., Rozendaal, N., and Jolles, J. (2002). Brain lesions in patients visiting a memory clinic with postconcussional sequelae after mild to moderate brain injury. J. Neuropsychiatry Clin. Neurosci. 14, 176–184.
58. Bagley, L.J., McGowan, J.C., Grossman, R.I., Sinson, G., Kotapka, M., Lexa, F.J., Berlin, J.A., and McIntosh, T.K. (2000). Magnetization transfer imaging of traumatic brain injury. J. Magn. Reson. Imaging 11, 1–8.
59. McGowan, J.C., Yang, J.H., Plotkin, R.C., Grossman, R.I., Umile, E.M., Cecil, K.M., and Bagley, L.J. (2000). Magnetization transfer imaging in the detection of injury associated with mild head trauma. AJNR Am. J. Neuroradiol. 21, 875–880.
60. Sinson, G., Bagley, L.J., Cecil, K.M., Torchia, M., McGowan, J.C., Lenkinski, R.E., McIntosh, T.K., and Grossman, R.I. (2001). Magnetization transfer imaging and proton MR spectroscopy in the evaluation of axonal injury: correlation with clinical outcome after traumatic brain injury. AJNR Am. J. Neuroradiol. 22, 143–151.
61. Mamere, A.E., Saraiva, L.A., Matos, A.L., Carneiro, A.A., and Santos, A.C. (2009). Evaluation of delayed neuronal and axonal damage secondary to moderate and severe traumatic brain injury using quantitative MR imaging techniques. AJNR Am. J. Neuroradiol. 30, 947–952.
62. Bergsneider, M., Hovda, D.A., McArthur, D.L., Etchepare, M., Huang, S.C., Sehati, N., Satz, P., Phelps, M.E., and Becker, D.P. (2001). Metabolic recovery following human traumatic brain injury based on FDG-PET: time course and relationship to neurological disability. J. Head Trauma Rehabil. 16, 135–148.
63. Eibner, C., Schell, T.L., and Jaycox, L.H. (2009). Care of war veterans with mild traumatic brain injury. N. Engl. J. Med. 361, 537.
64. Hoge, C.W., Goldberg, H.M., and Castro, C.A. (2009). Care of war veterans with mild traumatic brain injury—flawed perspectives. N. Engl. J. Med. 360, 1588–1591.
65. Sigford, B., Cifu, D.X. and Vanderploeg, R. (2009). Care of war veterans with mild traumatic brain injury. N. Engl. J. Med. 361, 536.
66. Ayling, E., Aghajani, M., Fouche, J.P., and van der Wee, N. (2012). Diffusion tensor imaging in anxiety disorders. Curr. Psychiatry Rep. 14, 197–202.
67. Broglio, S.P., Eckner, J.T., Surma, T., and Kutcher, J.S. (2011). Post-concussion cognitive declines and symptomatology are not related to concussion biomechanics in high school football players. J. Neurotrauma 28, 2061–2068.
68. Minoshima, S., Foster, N.L., Petrie, E.C., Albin, R.L., Frey, K.A., and Kuhl, D.E. (2002). Neuroimaging in dementia with Lewy bodies: metabolism, neurochemistry, and morphology. J. Geriatr. Psychiatry Neurol. 15, 200–209.
69. Minoshima, S., Sasaki, T., and Petrie, E. (2009). FDG PET imaging of dementia: principles and clinical applications, in: *Principles and Practice of PET and PET/CT.* R.L. Wahl (ed). Lippincott, Williams & Wilkins: Philadelphia, pps. 500–515.
70. Chappell, M.H., Ulug, A.M., Zhang, L., Heitger, M.H., Jordan, B.D., Zimmerman, R.D., and Watts, R. (2006). Distribution of microstructural damage in the brains of professional boxers: a diffusion MRI study. J. Magn. Reson. Imaging 24, 537–542.
71. Oishi, K., Andreia, F., van Zijl, P.C., Mori, S. (2011). *mRI Atlas of Human White Matter* 2nd ed. London, Academic Press.

Address correspondence to:
Eric C. Petrie, MD, MS
1660 S Columbian Way
Mail Code S-116 (MIRECC) VA Puget Sound
Seattle, WA 98108

E-mail: epetrie@uw.edu